

Gaussian functional approximation to 't Hooft's extension of the linear Σ model

Issei Nakamura

*McMaster University, Department of Physics and Astronomy,
1280 Main Street West, Hamilton, Ontario L8S 4L8, Canada; Present address: Division of Chemistry
and Chemical Engineering, California Institute of Technology, Pasadena, California 91125, USA*

V. Dmitrašinović

*Institute of Physics, Belgrade University, Pregrevača 118, Zemun, P.O.Box 57, 11080 Beograd, Serbia
(Received 22 July 2011; published 15 March 2012)*

We apply a self-consistent relativistic mean-field variational “Gaussian functional” (or optimized one-loop perturbation theory, or Hartree + RPA) approximation to the extended $N_f = 2$ linear σ model with spontaneously and explicitly broken chiral $SU_R(2) \times SU_L(2) \times U_A(1) \equiv O(4) \times O(2)$ symmetry. We set up the self-consistency, or gap equations that dress up the bare fields with “cactus tree” loop diagrams, and the Bethe-Salpeter equations that provide further dressing with one-loop irreducible diagrams. In a previous publication [V. Dmitrašinović and I. Nakamura, *J. Math. Phys. (N.Y.)* **44**, 2839 (2003).] we have already shown the ability of this approximation to create composite (i.e., bound and/or resonance) states. With explicit $SU_R(2) \times SU_L(2) \times U_A(1)$ chiral symmetry breaking first we consider how the $U_A(1)$ symmetry induced scalar-pseudoscalar meson mass relation that is known to hold in fermionic chiral models is modified by the bosonic gap equations. Then we solve the gap and Bethe-Salpeter equations numerically and discuss the solutions' properties and the particle content of the theory. We show that in the strong-coupling regime two, sometimes even three solutions to the η meson channel Bethe-Salpeter equation may coexist.

DOI: [10.1103/PhysRevD.85.056004](https://doi.org/10.1103/PhysRevD.85.056004)

PACS numbers: 11.30.-j, 11.30.Qc, 11.30.Rd

I. INTRODUCTION

Properties of the light scalar mesons are a long-standing puzzle in hadron-nuclear physics. It has been known at least since Ref. [1] that the $q\bar{q}$ scalar meson masses are largely determined by the explicitly broken $U_A(1)$ chiral symmetry of QCD. The $U_A(1)$ chiral symmetry breaking is not the only physical mechanism important for the scalar meson spectrum, however. Interactions of two pseudoscalar (isovector) mesons (pions) have long been suspected of providing some (most?) of the attractive strength in the (isoscalar) scalar channel. These pion-pion interactions are largely controlled by the $SU_L(2) \times SU_R(2)$ chiral symmetry. Explicit quark models with $SU_L(2) \times SU_R(2) \times U_A(1)$ chiral symmetry are ill-suited/too complicated for the study of meson-meson interactions, however, so one wishes to replace them with simpler chiral models that contain meson fields only.

One (simple) class of chiral models that contains the $SU_L(2) \times SU_R(2) \times U_A(1)$ chiral symmetry and its breaking as well as both the pseudoscalar and the scalar mesons is the linear sigma model [2], in its various forms, that depend on the number of (light) flavors N_f and the strength of the $U_A(1)$ chiral symmetry breaking. It is well known, however, that such models invariably “work” in the strong-coupling mode in order to reproduce the most basic observables, such as the meson masses. Moreover, such strong coupling of “elementary” mesons may lead to the dynamical formation of new scalar

resonances in the form of composite states of two pseudo-scalar mesons.

Manifestly, ordinary perturbation theory cannot be used for such purposes, so one must turn to nonperturbative methods that satisfy restrictions imposed by chiral symmetry. There are (relatively) few such methods, e.g., $1/N$ expansion [3], various N/D schemes [4], the optimized perturbation theory [5], the mean-field Hartree [6] + RPA [7], variational approximation based on the Gaussian functional ansatz [3,8,9], etc.). It turns out that most, if not all, of them are (closely) related, if not exactly equivalent to each other; for a detailed study of their relationships see Ref. [10]. In this paper we shall use the variational Gaussian functional approximation (GFA) because its chiral symmetry properties have been developed in perhaps the most explicit detail [11].

To this end we wish to continue the study of the three-flavor $U_L(3) \times U_R(3)$ symmetric linear sigma model [2,12,13] in the nonperturbative Gaussian functional approximation [14,15]. This model has a large number (18) of elementary spinless fields that lead to an even larger number of possible pairings in the Bethe-Salpeter (BS) equations. The study of their solutions necessarily involves a large number of coupled channel equations. Moreover, some of these equations are made even more complicated by the (further) mixing of the flavor singlet and the eighth member of the flavor octet.

For this reason we shall use here a linear sigma model that is simpler than Levy's full $N_f = 3$ version, viz., the

two-flavor 't Hooft model [16] that nevertheless still contains realistic $U_A(1)$ chiral symmetry breaking, but avoids the flavor-singlet-octet mixing. Its Lagrangian contains “only” eight, rather than 18 elementary boson fields, thus making the number of coupled channels in the BS equation manageable. We apply the variational Gaussian Functional Approximation to this model.

We emphasize here that we do not attempt to address the twin problems of the vacuum stability and high-energy behavior (“triviality”) of spinless field theories in Gaussian approximation (GA) [17–19] because the 'tHooft model is an effective low-energy field theory describing the interactions of mesons as bound states of quarks and antiquarks in the long-wavelength limit [1]. We assume that QCD, i.e., not the ϕ^4 interaction, controls the physics at high energies and thus ensures the stability of the vacuum. Exactly how this happens does not concern us here—the cutoff Λ is supposed to mimic the transition from the mesons to the quark-gluon d.o.f. in some (crude) way—it is the question of how these mesons interact at low and intermediate energies that interests us here.

We solve numerically the resulting gap and Bethe-Salpeter equations and discuss the particle content of the theory in this approximation. That allows us to study the effects of strong coupling on the scalar spectrum in some detail. That is where our most interesting results lie:

- (1) the solutions to the gap equation, i.e., the nonperturbatively dressed meson masses may, but need not depending on the values of certain bare coupling constants, satisfy a certain $U_A(1)$ chiral symmetry breaking induced mass relation that holds in the original quark model. The original [Nambu-Jona-Lasinio (NJL)] quark model predicts definite values of these coupling constants that lead to a (small) violation of the $U_A(1)$ mass relation, thus indicating that the boson loops tend to spoil/overtake some of the fermion-loop induced mass effects.
- (2) in certain regions of the coupling constant parameter space we find new (quasi/pseudo Nambu-Goldstone) meson bound states with exotic quantum numbers.
- (3) in the η meson (nonexotic) channel we find a proliferation of states with identical quantum numbers that accompanies the vanishing mass of the η meson (dynamical restoration of the $U_A(1)$ symmetry?) in the strong-coupling limit. Their masses are always comparable to, or larger than the cutoff Λ value, however, thus making them questionable as bona fide states.

Thus we have looked at the dynamically generated resonances in the parts of the spinless sector and found dynamically generated states. We expect that at least some of the flavor channels in the $N_f = 3$ model will be faithfully represented by this model, because the flavor-mixing

effects do not enter significantly into it. For this reason the present study of the 't Hooft model ought to be considered as a preparatory work for the full $N_f = 3$ calculation that has recently been restarted [15]. We hope that this work will ultimately lead to the clarification of the scalar meson spectroscopy, and, in particular, of the so-called σ meson problem.

This paper falls into five sections. After the Introduction, in Sec. II we introduce the linear Σ model. In Sec. III we outline the Gaussian approximation. In Sec. IV we solve numerically the gap and the Bethe-Salpeter equations and analyze the solutions. Finally we summarize and draw conclusions in Sec. V. A derivation of the Bethe-Salpeter equations in the pseudoscalar sector is given in Appendixes A and B.

II. THE 'T HOOFT MODEL

The original two-flavor Gell-Mann–Levy (GML) linear sigma model does not represent a realistic image of the spinless $q\bar{q}$ meson spectrum: this model maximally violates the $U_A(1)$ symmetry [1]. In response to this fact 't Hooft [16] extended the original GML linear sigma model [20] to include isovector scalar and isoscalar-pseudoscalar meson degrees of freedom [16].

The 't Hooft model consists of two coupled GML linear sigma models [20], one consisting of four light(er) (σ , $\boldsymbol{\pi}$) and the other of four heavier mesons (η , $\boldsymbol{\alpha}$). The light-meson sector consists of three massless pions and one massive isoscalar scalar meson, while the heavier-meson sector contains three heavy isovector scalar mesons and one lighter than these, but still heavy isoscalar-pseudoscalar meson. In the limit when the 't Hooft coupling, or mass m_{tH} is much heavier than any other mass scale in the problem, the heavy meson sector effectively decouples and the whole model is well approximated by the light sector. The latter is nothing but the Gell-Mann–Lévy linear sigma model, however. In this sense, we now understand how the GML linear sigma model can be both consistent with quark model and a good approximation to the chiral meson dynamics [2].

Both the Gell-Mann–Levy [20] and the 't Hooft [16] two-flavor model have the structure of an $O(N)$ sigma model. Each consists of chiral quartets: the GML model of one $O(4)$ multiplet, the 't Hooft model of two meson-quartets which can be “lined up” in one (broken) $O(8)$ symmetry multiplet. The latter model differs in one important respect from the former: the $U_A(1)$ symmetry is broken in a realistic manner. Admittedly it does not contain the full $SU(3)$ chiral symmetry, but the general features of this $SU(2)$ and the Levy $SU(3)$ model are identical. Bosonization of the chiral quark model leads to equality of the two quartic coupling constants $\lambda_1 = \lambda_2$ [1].

Definition of the model

The 't Hooft's [16] extension of the linear sigma model Lagrangian reads

$$\begin{aligned} \mathcal{L}_{\text{tH}} = & \text{Tr}(\partial_\mu M \partial^\mu M^\dagger + \mu_0^2 M M^\dagger) \\ & - \frac{1}{2}(\lambda_1 - \lambda_2)[\text{Tr}(M M^\dagger)]^2 - \lambda_2 \text{Tr}[(M M^\dagger)^2] \\ & + 2\kappa[e^{i\theta} \text{Det}M + \text{Det}M^\dagger] + \text{Tr}[H(M + M^\dagger)]. \end{aligned} \quad (1)$$

The meson field matrix M is a complex 2×2 matrix

$$M = T_a M_a = \frac{1}{\sqrt{2}}(\Sigma + i\Pi) = T_a(\sigma_a + i\pi_a), \quad (2)$$

composed of scalar Σ and pseudoscalar Π meson field quartets,

$$\Sigma = \frac{1}{\sqrt{2}}(\sigma + \boldsymbol{\alpha} \cdot \boldsymbol{\tau}) \quad \Pi = \frac{1}{\sqrt{2}}(\eta + \boldsymbol{\pi} \cdot \boldsymbol{\tau}). \quad (3)$$

where $T_a = \frac{1}{2}\tau_a$ are the generators of $U(2)$ with $\tau_0 = \mathbf{1}$ and $\tau_a, a = 1, 2, 3$ are the Pauli matrices. The four σ_a are the scalar fields ($\sigma, \boldsymbol{\alpha}$) and π_a are the pseudoscalar quartet ($\eta, \boldsymbol{\pi}$) fields.

Equation (1) is equivalent to the following

$$\begin{aligned} \mathcal{L}_{\text{tH}} = & \frac{1}{2}[(\partial_\mu \sigma)^2 + (\partial_\mu \boldsymbol{\pi})^2 + (\partial_\mu \eta)^2 + (\partial_\mu \boldsymbol{\alpha})^2] \\ & + \mathcal{L}_{\chi\text{SB}} + \frac{\mu_0^2}{2}[\sigma^2 + \boldsymbol{\pi}^2 + \eta^2 + \boldsymbol{\alpha}^2] \\ & + 2\kappa \cos\theta[\sigma^2 + \boldsymbol{\pi}^2 - \eta^2 - \boldsymbol{\alpha}^2] \\ & - 4\kappa \sin\theta[\sigma\eta - \boldsymbol{\pi} \cdot \boldsymbol{\alpha}] - \frac{\lambda_1}{8}[\sigma^2 + \boldsymbol{\pi}^2 + \eta^2 + \boldsymbol{\alpha}^2]^2 \\ & - \frac{\lambda_2}{2}[(\sigma\boldsymbol{\alpha} + \eta\boldsymbol{\pi})^2 + (\boldsymbol{\pi} \times \boldsymbol{\alpha})^2] \end{aligned} \quad (4)$$

which describes the dynamics of the two chiral meson quartets, ($\sigma, \boldsymbol{\pi}$) and ($\boldsymbol{\alpha}, \eta$), in this model, and $\lambda_1, \lambda_2, \kappa, \theta$ are the bare coupling constants (we keep here 't Hooft's original notation although other authors, see, e.g., Ref. [14] use a different definition of $\lambda'_2 \rightarrow \lambda_2, \lambda'_1 \rightarrow (\lambda_1 - \lambda_2)$, which may lead to confusion).

The 2×2 matrix H breaks the chiral $SU_L(2) \times SU_R(2)$ symmetry explicitly (thus inducing nonvanishing Nambu-Goldstone boson mass(es))

$$H = T_a h_a, \quad (5)$$

where h_a are the four explicit chiral symmetry breaking parameters. Only two (diagonal) ones, $a = (0, 3)$, are physically relevant and one, $a = 0$, is dominant. In this paper, we shall only study the case $h_0 \neq 0$, so that the isospin $SU(2)$ symmetry remains conserved. Thus, the explicit chiral symmetry breaking (χSB) term in the Lagrangian Eq. (4) is

$$\mathcal{L}_{\chi\text{SB}} = -\mathcal{H}_{\chi\text{SB}} = \varepsilon\sigma, \quad (6)$$

as suggested by the underlying QCD theory and/or chiral quark model. This term also gives the η meson a nonvanishing mass that breaks the $U_A(1)$ symmetry, but this breaking is insufficient, as in that case one finds $m_\pi = m_\eta$.

In order to account for $m_\pi \neq m_\eta$, we must introduce the nonvanishing coupling κ that leads to (further) explicit breaking of the $O(2) \simeq U_A(1)$ symmetry. As there are no states in the isotriplet that can mix with the isosinglet in the good isospin limit, there is no mixing problem in this model, in contrast to the $SU(3)$ version of the σ model. Any nonvanishing value of the angle θ leads to the explicit (not spontaneous) CP violation in this model, so we set it equal to zero. Then the only effect of the $U_A(1)$ symmetry breaking interaction in the 't Hooft model is the meson mass shift [1]:

$$m_\eta^2 - m_\pi^2 = -[m_\sigma^2 - m_a^2].$$

Thus we see that the 't Hooft model consists of two coupled Gell-Mann-Lévy (GML) linear sigma models [20], one with a light and the other with a heavy quartet of mesons. The next question is: Do the bosonic loop effects enhance or decrease this meson mass splitting? Does it change this mass "sum rule"? To answer these questions we must develop the GA to the 't Hooft model.

Note that the symmetries of the various parts of the interaction Lagrangian also vary: (i)

$$\lambda_1 \neq 0; \lambda_2 = \kappa = \theta = 0 \quad (7)$$

implies $O(8)$ symmetry. (ii)

$$\lambda_1 \neq 0 \neq \lambda_2; \kappa = \theta = 0 \quad (8)$$

implies $O(4) \times O(2)$ symmetry. (iii)

$$\lambda_1 \neq 0 \neq \lambda_2; \kappa \neq 0 = \theta \quad (9)$$

implies $O(4)$ symmetry and the number of Nambu-Goldstone bosons must change accordingly.

We may rewrite the Lagrangian Eq. (4) in the following "shorthand notation" form which will turn out useful later

$$\begin{aligned} \mathcal{L}(\sigma_a, \pi_a) = & \frac{1}{2}[\partial_\mu \sigma_a \partial^\mu \sigma_a + \partial_\mu \pi_a \partial^\mu \pi_a] \\ & + \frac{1}{2}\mu_0^2(\sigma_a \sigma_a + \pi_a \pi_a) \\ & - 2\mathcal{H}_{abcd} \sigma_a \sigma_b \pi_c \pi_d + h_a \sigma_a \\ & - \frac{1}{3}\mathcal{F}_{abcd}(\sigma_a \sigma_b \sigma_c \sigma_d + \pi_a \pi_b \pi_c \pi_d). \end{aligned} \quad (10)$$

where $h_a \sigma_a = \varepsilon\sigma$. The coefficients \mathcal{F}_{abcd} and \mathcal{H}_{abcd} are given by

$$\begin{aligned} \mathcal{F}_{abcd} = & \frac{\lambda_1}{8}(\delta_{ab}\delta_{cd} + \delta_{ad}\delta_{bc} + \delta_{ac}\delta_{bd}) + \frac{\lambda_2}{2}\delta_{0a}\delta_{0b}\delta_{ic}\delta_{id} \\ \mathcal{H}_{abcd} = & -\frac{\lambda_1}{8}\delta_{ab}\delta_{cd} + \lambda_2\left(\delta_{0a}\delta_{0c}\delta_{bi}\delta_{di} + \frac{1}{2}\varepsilon_{bci}\varepsilon_{iad}\right). \end{aligned} \quad (11)$$

Here the indices a, b, c, d run from 0 to 3, and indices i, j run from 1 to 3.

III. THE GAUSSIAN VARIATIONAL METHOD

The linear sigma model is a strongly interacting renormalizable quantum field theory; due to the size of the self-interaction coupling constant(s) the perturbative approximations seem to be inapplicable. Therefore, a nonperturbative approximation, such as the Gaussian functional one, that is equivalent to the resummation of certain infinite classes of Feynman diagrams that are unitary and causal [3,9,10], [21,22] is called for.

In this paper we apply the chirally invariant, Lorentz invariant self-consistent mean-field variational approximation [Gaussian functional approximation] [3,8,9] to the extended ('t Hooft) linear sigma model. The major improvement that we bring forward in this paper is the correct implementation of the chiral symmetry in this nonperturbative approximation. For that purpose we have proven the chiral Ward-Takahashi identities, among them the Nambu-Goldstone theorem, the Dashen relation and the axial current (partial) conservation (PCAC) in this

approximation [10,22]. This method sometimes also goes under the names of self-consistent mean-field approximation (MFA), or Hartree + RPA. In the following we shall treat these two terms as if they were synonymous. The GFA consists of two parts: 1) the (Hartree) energy minimization, or gap equations; and 2) the two-body, or Bethe-Salpeter, or RPA equations of motion. Each one of these steps leads to an effective change (dressing) of particle masses/self-energies.

The basic question is: Does the first meson dressing due to the gap equation in the GFA enhance or decrease the U(1) induced scalar meson splitting? Does the second dressing produce new scalar, or pseudoscalar states? To answer these questions we must develop the GFA to the 't Hooft model.

A. The Gaussian functional approximation

We use the Gaussian ground state (“vacuum”) functional Ansatz

$$\Psi_0[\vec{\phi}] = \mathcal{N} \exp\left(-\frac{1}{4\hbar} \int d\mathbf{x} \int d\mathbf{y} (\pi_a(\mathbf{x}) G_{ab}^{-1}(\mu_{a\pi}; \mathbf{x}, \mathbf{y}) \pi_b(\mathbf{y}) + [\sigma_a(\mathbf{x}) - \langle \sigma_a(\mathbf{x}) \rangle] G_{ab}^{-1}(M_{a\sigma}; \mathbf{x}, \mathbf{y}) [\sigma_b(\mathbf{y}) - \langle \sigma_b(\mathbf{y}) \rangle])\right), \quad (12)$$

where \mathcal{N} is the normalization constant, $\langle \sigma_a(\mathbf{x}) \rangle = \bar{\sigma}_a$ is the vacuum expectation value (v.e.v.) of the a -th scalar field, which we shall henceforth assume to be translationally invariant $\langle \sigma_a(\mathbf{x}) \rangle = \langle \sigma_a(0) \rangle \equiv \langle \sigma_a \rangle$ and

$$G_{ab}(m_a; \mathbf{x}, \mathbf{y}) = \frac{1}{2} \delta_{ab} \frac{d\mathbf{k}}{(2\pi)^3} \frac{1}{\sqrt{\mathbf{k}^2 + m_a^2}} e^{i\mathbf{k}\cdot(\mathbf{x}-\mathbf{y})}. \quad (13)$$

Here we have assumed conservation of the parity symmetry of the vacuum, i.e., that the pseudoscalar fields have vanishing v.e.v.s: $\langle \pi_a \rangle = 0$. Furthermore, note that we have explicitly kept \hbar (while setting the velocity of light $c = 1$) to keep track of quantum corrections and count the number of “loops” in our calculation. Finally the vacuum energy density/effective potential can be written in shorthand notation as

$$\mathcal{E}(\mu_{a\pi}, M_{a\sigma}, \langle \sigma_a \rangle = \bar{\sigma}_a) = \langle \Psi_0 | \mathcal{H} | \Psi_0 \rangle \quad (14)$$

$$\begin{aligned} &= \frac{1}{2} \mu_0^2 \bar{\sigma}_a^2 + \frac{1}{4} \{G_{ab}^{-1}(M_\sigma) + G_{ab}^{-1}(\mu_\pi)\} - \frac{1}{2} (\mu_0^2 + M_{\sigma_a}^2) G_{ab}(M_{\sigma_a}) \\ &\quad - \frac{1}{2} (\mu_0^2 + \mu_{\pi_a}^2) G_{ab}(\mu_\pi) + 2\mathcal{H}_{abcd} \{G_{ab}(\mu_\pi) \bar{\sigma}_c \bar{\sigma}_d + G_{ab}(\mu_\pi) G_{cd}(M_\sigma)\} \\ &\quad + \frac{1}{3} \mathcal{F}_{abcd} \{\bar{\sigma}_a \bar{\sigma}_b \bar{\sigma}_c \bar{\sigma}_d + 6\bar{\sigma}_a \bar{\sigma}_b G_{cd}(M_\sigma) + 3G_{ab}(M_\sigma) G_{cd}(M_\sigma) + 3G_{ab}(\mu_\pi) G_{cd}(\mu_\pi)\} - h_a \bar{\sigma}_a. \end{aligned} \quad (15)$$

where

$$I_0(m_a) = \frac{1}{2} \int \frac{d\mathbf{k}}{(2\pi)^3} \frac{1}{\sqrt{\mathbf{k}^2 + m_a^2}} = i \int \frac{d^4 k}{(2\pi)^4} \frac{1}{k^2 - m_a^2 + i\epsilon} = G_{aa}(\mathbf{x}, \mathbf{x}) \quad (16)$$

$$I_1(m_a) = \frac{1}{2} \int \frac{d\mathbf{k}}{(2\pi)^3} \sqrt{\mathbf{k}^2 + m_a^2} = -\frac{i}{2} \int \frac{d^4 k}{(2\pi)^4} \log(k^2 - m_a^2 + i\epsilon) + \text{const.} = G^{-1}(\mathbf{x}, \mathbf{x}). \quad (17)$$

We identify $\hbar I_1(m_a)$ with the familiar “zero-point” energy density of a free spinless field of mass m_a .

The divergent integrals $I_{0,1}(m_a)$ are understood to be regularized via an UV momentum cutoff Λ . Thus we have introduced a new free parameter into the calculation. This was bound to happen in one form or another, since even in the renormalized perturbation theory one must introduce a new dimensional quantity (the “renormalization scale/point”) at the one-loop level. We treat this model as an effective theory and thus keep the cutoff without renormalization.

B. The energy minimization, or gap equations in 't Hooft model

In order to minimize the energy density, we take the first derivatives of the energy density Eq. (14) with respect to the field vacuum expectation values $\langle\sigma_a\rangle = \bar{\sigma}_a$ and the “dressed” masses $\mu_{a\pi}$, $M_{a\sigma}$ and set them equal to zero:

$$\left(\frac{\partial\mathcal{E}(\mu_{a\pi}, M_{a\sigma}, \bar{\sigma}_a)}{\partial\bar{\sigma}_b}\right)_{\min} = 0; b = 0, \dots, 3; \quad (18)$$

$$\left(\frac{\partial\mathcal{E}(\mu_{a\pi}, M_{a\sigma}, \bar{\sigma}_a)}{\partial\mu_{b\pi}}\right)_{\min} = 0; b = 0, \dots, 3; \quad (19)$$

$$\left(\frac{\partial\mathcal{E}(\mu_{a\pi}, M_{a\sigma}, \bar{\sigma}_a)}{\partial M_{b\sigma}}\right)_{\min} = 0; b = 0, \dots, 3. \quad (20)$$

These are not sufficient conditions for the (local) minimization, however, but merely necessary. In other words they ensure that only their solutions are extrema or saddle points of the energy. For absolute minimization one needs the second variation of the energy to be positive. Then, one must compare the actual values of the energy at all such local minima in order to find the absolute one.

So the first question is when are these extrema/saddle points actual (local) minima, i.e., when is the sign of the second variation of the energy positive? This question has already been dealt with in Ref. [17] in the case of single component fields, i.e., with no spontaneously broken internal symmetry. The case with multiple fields is not fundamentally different from the single field case: the main technical difference is that one has a matrix of second derivatives rather than individual ones. Positivity of such a matrix is ensured by the positivity of (all of) its principal minors. One can show that this condition is related to the twin requirements of a) positivity of the mass-squared matrix, and b) positivity of the (renormalized) coupling constants. The latter is tantamount to avoiding the Landau ghost singularity at all values of momenta. As this Lagrangian does not lead to asymptotic freedom, its Landau ghosts lie at high (rather than low) momenta. Stevenson *et al.* [18,19] have shown that, as a consequence of such a Landau ghost, one finds another (infinitely deep) minimum of the energy in the limit when the v.e.v. goes to infinity/grows without bounds. Thus the problem of stability of the vacuum is closely related to the high-energy

behavior of the theory, which we have expressly decided to avoid, due to the effective nature of the present model.

Equations (18)–(20), determine the dressed masses $\mu_{a\pi}$, $M_{a\sigma}$ and the vacuum expectation values of the meson fields $\langle\sigma_a\rangle = \bar{\sigma}_a$ and sometimes go by the name of gap equations for scalar and pseudoscalar mesons. The first set of energy minimization Eqs. (18) is given in shorthand notation by

$$h_a = m^2\bar{\sigma}_a + 4\mathcal{H}_{abcd}\bar{\sigma}_b G_{cd}(m_\pi) + \frac{1}{3}\mathcal{F}_{abcd}[4\bar{\sigma}_b\bar{\sigma}_c\bar{\sigma}_d + 12\bar{\sigma}_b G_{cd}(m_\sigma)]. \quad (21)$$

or, in the longhand notation

$$\varepsilon = -v(\mu_0^2 + 4\kappa) + \frac{\lambda_1}{2}v[v^2 + 3I_0(M_\sigma) + 3I_0(M_\alpha) + 3I_0(\mu_\pi) + I_0(\mu_\eta)] + 3\lambda_2vI_0(M_\alpha) \quad (22)$$

$$v = \langle\sigma_0\rangle; \quad \langle\alpha_i\rangle = 0, \quad i = 1, 2, 3; \\ \langle\pi_a\rangle = 0, \quad a = 0, 1, 2, 3, \quad (23)$$

where the divergent integral $I_0(m_i)$ given by Eq. (16) is understood to be regularized via an UV momentum cut off Λ , either three-, or four-dimensional.

Equations (22) and (23) can be identified as truncated Schwinger-Dyson (SD) equations [8] for the one-point Green function, see Fig. 1. We associate the nonvanishing vacuum expectation value (v.e.v.) with the “sigma meson” field ϕ_0 , whose apparent mass equals $m_0 = M_\sigma$, and the remaining seven fields’ $\langle\sigma_a\rangle = 0; a = 1, 2, 3$ and $\langle\pi_a\rangle = 0; a = 0, 1, 2, 3$.

The second set of energy minimization Eqs. (19) in shorthand notation are

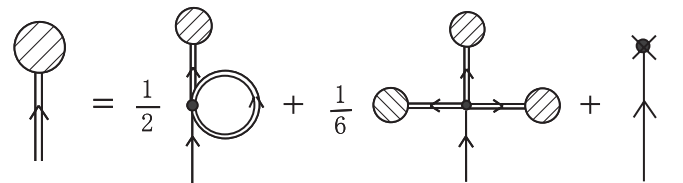


FIG. 1. One-point Green function Schwinger-Dyson equation determining the dynamics of the σ model in the Hartree approximation: the one-loop graph (a), and the tree tadpole diagram (b). The solid line denotes the bare meson multiplet, double solid line is the dressed meson multiplet. The shaded blob together with the double line leading to it (the “tadpole”) denotes the vacuum expectation value of the field (i.e., the one-point Green function) and the solid dot in the intersection of four lines denotes the bare four-point coupling. Diagrams are explicitly multiplied by their symmetry numbers.

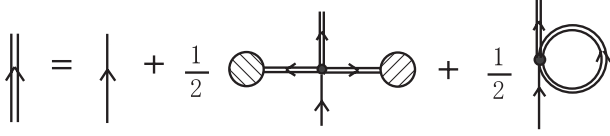


FIG. 2. Two-point Green function Schwinger-Dyson equation: the one-loop graph (a), the tree tadpole diagram (b). The symbols have the same meaning as in Fig. 1.

$$\begin{aligned}
(M_S^2)_{ab} &= -\mu_0^2 \delta_{ab} - 4\kappa(\delta_{a0}\delta_{b0} - \delta_{ai}\delta_{bi}) \\
&\quad + 4\mathcal{F}_{abcd}\bar{\sigma}_c\bar{\sigma}_d + 4\mathcal{F}_{abcd}G_{cd}(M_\sigma) \\
&\quad + 4\mathcal{H}_{abcd}G_{cd}(\mu_\pi), (\mu_P^2)_{ab} \\
&= -\mu_0^2 \delta_{ab} + 4\kappa(\delta_{a0}\delta_{b0} - \delta_{ai}\delta_{bi}) \\
&\quad + 4\mathcal{H}_{abcd}\bar{\sigma}_c\bar{\sigma}_d + 4\mathcal{H}_{abcd}G_{cd}(M_\sigma) \\
&\quad + 4\mathcal{F}_{abcd}G_{cd}(\mu_\pi). \tag{24}
\end{aligned}$$

or in longhand notation

$$\begin{aligned}
M_\sigma^2 &= -\mu_0^2 - 4\kappa + \frac{3\lambda_1}{2}v^2 + \frac{\lambda_1}{2}[3I_0(M_\sigma) + 3I_0(M_\alpha) \\
&\quad + 3I_0(\mu_\pi) + I_0(\mu_\eta)] + 3\lambda_2 I_0(M_\alpha) \tag{25}
\end{aligned}$$

$$\begin{aligned}
M_\alpha^2 &= -\mu_0^2 + 4\kappa + \left(\frac{\lambda_1}{2} + \lambda_2\right)v^2 \\
&\quad + \frac{\lambda_1}{2}[I_0(M_\sigma) + 5I_0(M_\alpha) + 3I_0(\mu_\pi) + I_0(\mu_\eta)] \\
&\quad + \lambda_2[I_0(M_\sigma) + 2I_0(\mu_\pi)] \tag{26}
\end{aligned}$$

$$\begin{aligned}
\mu_\pi^2 &= -\mu_0^2 - 4\kappa + \frac{\lambda_1}{2}v^2 + \frac{\lambda_1}{2}[I_0(M_\sigma) + 3I_0(M_\alpha) \\
&\quad + 5I_0(\mu_\pi) + I_0(\mu_\eta)] + \lambda_2[I_0(\mu_\eta) + 2I_0(M_\alpha)] \tag{27}
\end{aligned}$$

$$\begin{aligned}
\mu_\eta^2 &= -\mu_0^2 + 4\kappa + \frac{\lambda_1}{2}v^2 + \frac{\lambda_1}{2}[I_0(M_\sigma) + 3I_0(M_\alpha) \\
&\quad + 3I_0(\mu_\pi) + 3I_0(\mu_\eta)] + 3\lambda_2 I_0(\mu_\pi) \tag{28}
\end{aligned}$$

where the divergent integral $I_0(m_i)$ is given by Eq. (16) and (25)–(28). also have a Feynman-diagrammatic interpretation shown in Fig. 2.

Upon inserting Eq. (22) into Eqs. (25)–(28) one finds the following four gap equations:

$$M_\sigma^2 = \frac{\varepsilon}{v} + \lambda_1 v^2 \tag{29}$$

$$\begin{aligned}
M_\alpha^2 &= \frac{\varepsilon}{v} + \lambda_2 v^2 + 8\kappa + \lambda_1[I_0(M_\alpha) - I_0(M_\sigma)] \\
&\quad + \lambda_2[I_0(M_\sigma) + 2I_0(\mu_\pi) - I_0(M_\alpha)] \tag{30}
\end{aligned}$$

$$\begin{aligned}
\mu_\pi^2 &= \frac{\varepsilon}{v} + \lambda_1[I_0(\mu_\pi) - I_0(M_\sigma)] + \lambda_2[I_0(\mu_\eta) - I_0(M_\alpha)] \\
&\tag{31}
\end{aligned}$$

$$\begin{aligned}
\mu_\eta^2 &= \frac{\varepsilon}{v} + 8\kappa + \lambda_1[I_0(\mu_\eta) - I_0(M_\sigma)] \\
&\quad + 3\lambda_2[I_0(\mu_\pi) - I_0(M_\alpha)] \tag{32}
\end{aligned}$$

Let us now look at various symmetry limits:

- (1) If we take the $\lambda_2 \rightarrow 0$ and $\kappa \rightarrow 0$ limit, the solutions to the gap equations Eqs. (31) and (32) become degenerate $\mu_\eta^2 = \mu_\pi^2 = M_\alpha^2$, whereas the solution to the gap equation Eq. (29) M_σ^2 remains distinct. This is the $O(8)$ symmetry limit. One might be tempted to identify μ_π with the physical pion mass, and M_σ with the physical σ mass, then solve these equations and stop there. However, with $\varepsilon = 0$ these equations admit only massive solutions $M_\sigma > \mu_\pi > 0$ for real, positive values of λ_1 , μ_0^2 and any real ultraviolet cut off Λ in the momentum integrals $I_{0,1}(m_i)$ as these are positive definite (for any real mass). In other words the ‘‘pion’’ π_a , ($a = 1, 2, 3$) excitations are massive, with mass $\mu_\pi \neq 0$, in MFA, even in the chiral limit. This looks like a breakdown of the $O(4)$ invariance of this method, but, as discussed at length in Ref. [21], there is a solution via the Bethe-Salpeter equation.¹
- (2) In the $\lambda_2 \neq 0$ limit, while keeping $\kappa \rightarrow 0$, the solutions to the gap equations Eqs. (31) and (32) are degenerate $\mu_\eta^2 = \mu_\pi^2$, whereas the solution to the gap equations Eq. (29) M_σ^2 and Eq. (30) M_α^2 remain distinct. This is the $O(4) \times O(2)$ symmetry limit.
- (3) In the $\lambda_2 \rightarrow 0$ limit, while keeping $\kappa \neq 0$, the solutions to the gap equations, if they indeed exist, do not satisfy the same $U(1)$ sum rule.

To see the problem with the existence of solutions to the gap equation in this case, just look at the mass differences

$$M_\alpha^2 - \mu_\eta^2 = \lambda_1[I_0(M_\alpha) - I_0(\mu_\eta)] \tag{33}$$

$$M_\alpha^2 - M_\sigma^2 = 8\kappa - \lambda_1 v^2 + \lambda_1[I_0(M_\alpha) - I_0(M_\sigma)] \tag{34}$$

$$\mu_\eta^2 - \mu_\pi^2 = 8\kappa + \lambda_2[I_0(\mu_\eta) - I_0(\mu_\pi)] \tag{35}$$

Equation (33) is inconsistent with the inequality $M_\alpha^2 > \mu_\eta^2$, at least with the three-dimensional regularization of I_0 . Therefore, we must let $\lambda_2 \neq 0$.

(3) If we take the $\lambda_1 \rightarrow \lambda_2$ limit, while keeping $\kappa \neq 0$, all of the solutions to the gap equations Eqs. (29)–(32) remain distinct $\mu_\eta^2 \neq M_\alpha^2 \neq M_\sigma^2 \neq \mu_\pi^2$. It is interesting to note that these solutions still satisfy the same (Born level) sum rule

$$\mu_\eta^2 - \mu_\pi^2 = -[M_\sigma^2 - M_\alpha^2] \tag{36}$$

¹It is well known in the quantum many-body literature that the Hartree, or mean-field approximation does not respect internal symmetries. The corrective measure goes by the name of random phase approximation (RPA).

so long as $\lambda_1 = \lambda_2$ holds. Consequently,

$$\mu_\eta^2 + M_\sigma^2 = \mu_\pi^2 + M_\alpha^2 \quad (37)$$

and the two isoscalar-pseudoscalar channels have nearby (if not identical) thresholds:

$$(\mu_\eta + M_\sigma)^2 \simeq (\mu_\pi + M_\alpha)^2 \quad (38)$$

Before proceeding to solve the gap Eqs. (29)–(32), we will have to determine the value of the ε parameter in terms of observables calculated in the Gaussian approximation. For this purpose we will also have to use the Bethe-Salpeter equation.

C. The Bethe-Salpeter equation in the pseudoscalar sector

In Ref. [11,21] we have shown that the Nambu-Goldstone particles appear as poles in the *two-particle propagator*, i.e., they are bound states of the two distinct massive elementary excitations in the theory.

We specify the two-body dynamics in the theory in terms of the four-point SD equation or, equivalently, of the Bethe-Salpeter equation, see Figs. 3 and 4. Here we shall simply state the correct form of the four-point SD equation based on the truncation of the exact SD equation [8]. The derivation from the Gaussian approximation, in the symmetric phase of the theory can be found in Ref. [3]. The corresponding derivation in the asymmetric (Nambu-Goldstone) phase can be found in Ref. [6]. Moreover, this BS equation is the ‘‘random phase approximation’’ (RPA) equation of motion that describe ‘‘quasiparticles’’ in this theory, see Ref. [6,7].

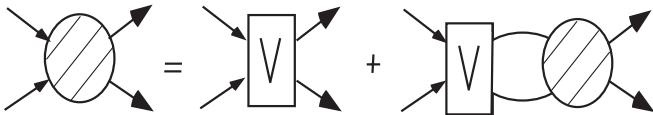


FIG. 3. Four-point Green function Schwinger-Dyson, or Bethe-Salpeter equation. The square ‘‘box’’ represents the potential, whereas the round ‘‘blob’’ is the BS amplitude itself. All lines are meant as dressed fields, i.e., as double lines in Figs. 1 and 2.

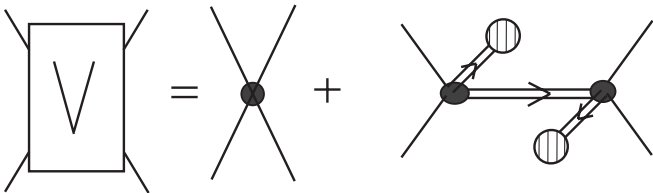


FIG. 4. The potential (square box) entering the Bethe-Salpeter equation, as defined in the RPA.

IV. NUMERICAL SOLUTIONS

A. The self-consistency, or gap equation

Having determined the value of the parameter $\varepsilon = \nu m_\pi^2$ in terms of observables, one can solve the gap equations. We fix the v.e.v. ν at the pion decay constant f_π value of 93 MeV and the physical pion mass at $m_\pi = 140$ MeV and let $\lambda_1 \rightarrow \lambda_2$. Thus the system of gap Eqs. (29)–(32) turns into four equations:

$$\lambda_1 = \lambda_2 = \left(\frac{M_\sigma^2 - \frac{\varepsilon}{\nu}}{\mu_\pi^2 - \frac{\varepsilon}{\nu}} \right) = \left(\frac{M_\sigma^2 - m_\pi^2}{\mu_\pi^2 - m_\pi^2} \right) \quad (39)$$

$$\nu^2 = f_\pi^2 = \left(\frac{M_\sigma^2 - \frac{\varepsilon}{\nu}}{\mu_\pi^2 - \frac{\varepsilon}{\nu}} \right) [I_0(\mu_\pi) - I_0(M_\sigma) + I_0(\mu_\eta) - I_0(M_\alpha)] \quad (40)$$

$$M_\alpha^2 - M_\sigma^2 = 8\kappa + 2 \left(\frac{M_\sigma^2 - \frac{\varepsilon}{\nu}}{\mu_\pi^2 - \frac{\varepsilon}{\nu}} \right) [I_0(\mu_\pi) - I_0(M_\alpha)] \quad (41)$$

$$\mu_\eta^2 - \mu_\pi^2 = 8\kappa + 2 \left(\frac{M_\sigma^2 - \frac{\varepsilon}{\nu}}{\mu_\pi^2 - \frac{\varepsilon}{\nu}} \right) [I_0(\mu_\pi) - I_0(M_\alpha)] \quad (42)$$

As noted earlier, the $U_A(1)$ mass sum rule

$$\mu_\eta^2 - \mu_\pi^2 = -[M_\sigma^2 - M_\alpha^2] \quad (43)$$

reduces the number of independent equations to three. We fix the values of $\lambda_1 = \lambda_2$, $\nu = f_\pi$ and κ that leaves us with three equations with three variables, which may be chosen at will from the four masses μ_η , μ_π , M_σ , M_α , while taking into account the $U_A(1)$ sum rule. So, if one fixes one of the three independent masses, e.g., μ_η , one ends up with two equations with two unknowns. Moreover, note that one more parameter, in this case the cutoff Λ , remains free. This leads to a set of equations that can be solved just as in the GML limit [22].

Here we use $I_0(m)$ Eq. (16) as the basic integral to be regulated. We show here the results for the ‘‘covariant’’/Euclidean four-dimensional Euclidean cutoff regularization of this quadratically divergent integral

$$I_0^{(4)}(m^2) = (4\pi)^{-2} m^2 [x_4 - \ln(1 + x_4)]; \quad x_4 = \left(\frac{\Lambda_4}{m} \right)^2. \quad (44)$$

Note that the $\lambda_1 = \lambda_2$ condition leads towards a reduction of the degree of divergence in the gap equations, *viz.* for $\lambda_1 \neq \lambda_2$ one has

$$\mu_\eta^2 - \mu_\pi^2 + [M_\sigma^2 - M_\alpha^2] = 0 = (\lambda_1 - \lambda_2) [v^2 - I_0(M_\alpha) + I_0(M_\sigma) + I_0(\mu_\eta) - I_0(\mu_\pi)] \quad (45)$$

where the leading quadratic divergences cancel in the sum/difference.

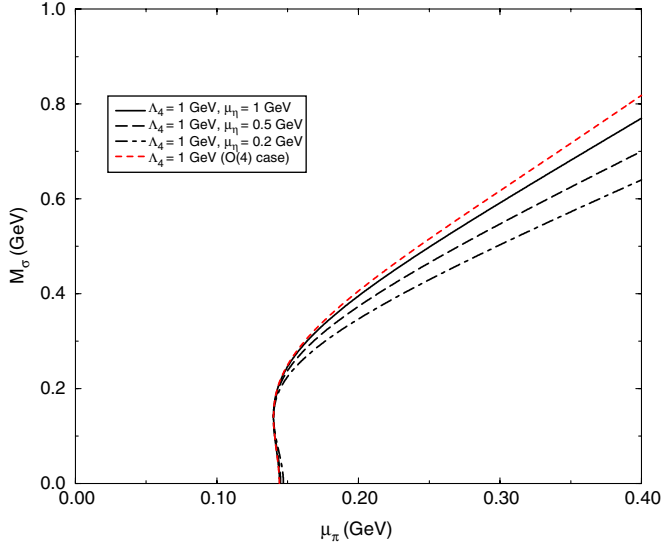


FIG. 5 (color online). Solutions to the nonchiral gap equation in the Gaussian approximation to the 't Hooft linear sigma model with different values of the four-dimensional cutoff Λ_4 , while keeping the μ_η mass fixed at 0.7 GeV, i.e., slightly above its physical value of 600 MeV.

Numerical solutions to the Eqs. (39)–(42) are shown in Figs. 5 and 6, for various cutoff Λ and mass μ_η .

Every point on the (M_σ, μ_π) curve represents a solution to the gap equation, thus signalling the existence of a degree of freedom in the form of one continuous (free) parameter. This free parameter can be related to the bare coupling constant λ_1 by Eq. (25), for every (M_σ, μ_π) pair.

In Fig. 5 we see that with increasing cutoff Λ all solutions to the gap equation approach the symmetry

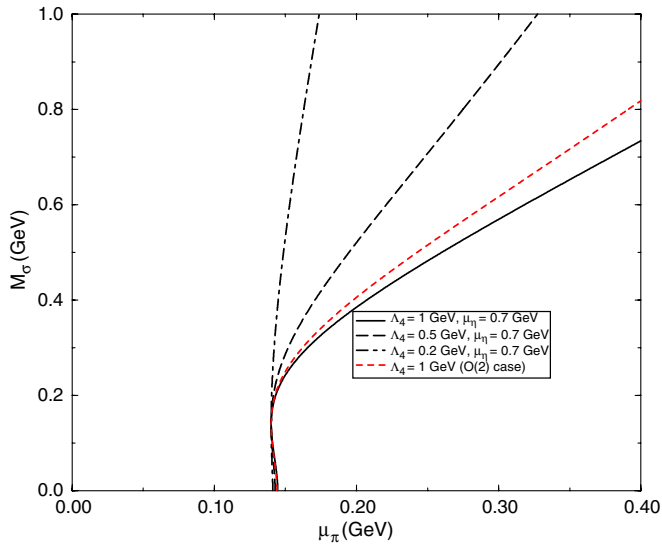


FIG. 6 (color online). Solutions to the nonchiral gap equation in the Gaussian approximation to the 't Hooft linear sigma model with different values of the μ_η mass, while keeping the four-dimensional cutoff Λ_4 fixed at 1 GeV.

restoration limit $M_\sigma \rightarrow \mu_\pi$ for large values of M_σ , or equivalently large λ_1 . This means that the large boson loop effects lead to chiral symmetry restoration, in contrast to the fermion loops which lead to symmetry breaking.

Moreover, as can be seen in Fig. 6, the solutions to the 't Hooft model gap equations approach (slowly) the GML model limit [22], as the $U_A(1)$ symmetry breaking is increased, i.e., as $\mu_\eta \rightarrow \infty$, denoted as the O(4) symmetry case in Fig. 6.

Thus we have shown that we can smoothly recover the old GML model results Ref. [22]. Just as in the GML model case, these “single-particle Hartree” masses are not the physical ones. To obtain the physical masses one must solve the (two-body) Bethe-Salpeter equations.

B. The Bethe-Salpeter Equation for the η meson mass

We reduced solving the BS equations in the isoscalar-pseudoscalar channel to solving a single algebraic equation Eq. (B6) involving transcendental analytic functions $I_{M\mu}(s)$ with branch cuts at and imaginary parts above the corresponding thresholds. There are two such branch cuts, as there are two thresholds: (σ, η) and (π, α) whose numerical values are determined by the gap equations. The BS mass equation has in general both the real and the imaginary part: for η mass values lying below the lowest two-body threshold only the real part is relevant; for heavier η masses one must take the imaginary part into account as well.

From numerical solutions to the real part of Eq. (B6) one can see that the η mass is always shifted *downward* from the elementary η field's mass μ_η , in agreement with the variational property of the mean-field approximation.

With increasing coupling constant λ_1 the solution to the η mass BS equation solution increases above the $M\mu$ threshold and the bare and dressed components of the wave function cannot be separated any more. Then the state itself must be considered as predominantly a meson-meson composite [23].

In Figs. 7–9 we see that there is at first only one, then three and finally two solutions. There one can see that the η mass changes continuously with decreasing coupling λ_1 and connects smoothly to the perturbative σ mass M_σ in the weak coupling limit. (One must keep in mind that increasing M_σ implies increasing the (bare) quartic coupling $\lambda_1 = \lambda_2$, while keeping the pion decay constant v fixed at its experimental value 93 MeV.) The lowest (mass) branch corresponds to the usual “physical” (the quotation marks here only mean that this η meson does not exist in the PDG tables) mass, but it disappears for sufficiently large M_σ . The two upper branches are novel effects: They appear at, or near new thresholds (in this case at the $\sigma - \eta$ and $\alpha - \pi$ ones), and the lower one may be a bound state. We have taken drastically different values of the Λ_4/μ_η ratio so as to make sure that this is not an

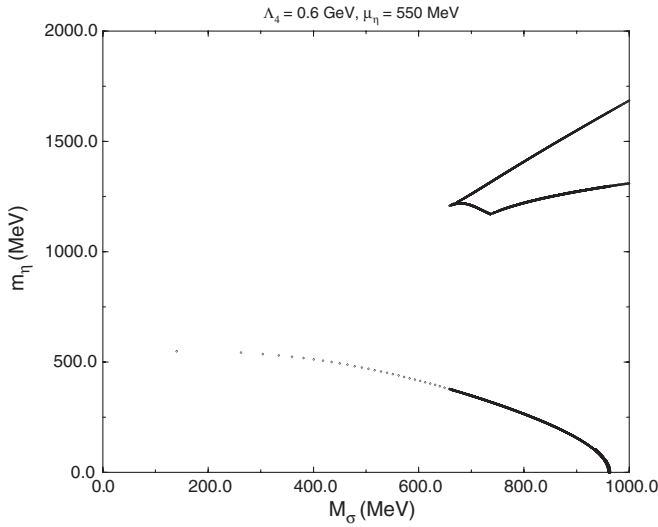


FIG. 7. Isoscalar-pseudoscalar η meson mass (solution to the BS eqs. with $\Lambda_4 = 0.6$ GeV and $\mu_\eta = 550$ MeV) m_η as a function of the scalar mass M_σ in the 't Hooft model.

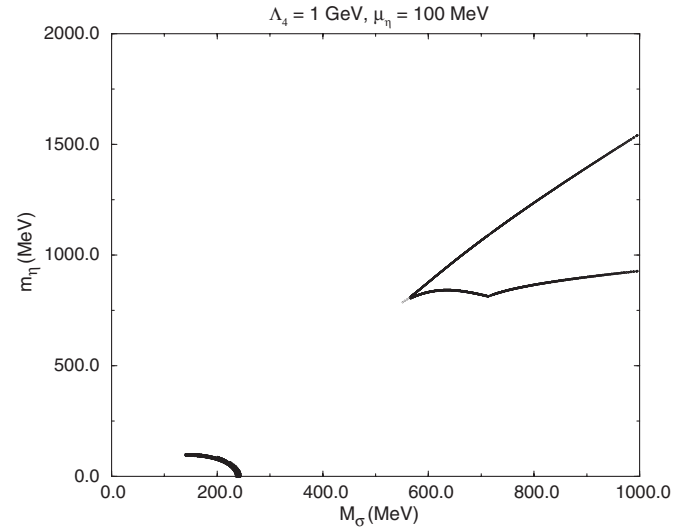


FIG. 9. Isoscalar-pseudoscalar η meson mass (solution to the BS eqs. with $\Lambda_4 = 1.0$ GeV and $\mu_\eta = 100$ MeV) m_η as a function of the scalar mass M_σ in the 't Hooft model.

artifact of the cutoff procedure: Figs. 7–9 clearly show that the same structure appears for all three values of Λ_4/μ_η . Their masses appear to scale with the cutoff Λ_4 , however, at least in the region studied here, so that the question of their physical significance may rightfully be raised.

In order to understand the particle content of this approximation we employ the Kallen-Lehmann spectral function [10,23]. The lower of the two dynamical poles lies below the $\alpha - \pi$ and $\sigma - \eta$ thresholds and is therefore a bound state that appears as a Dirac delta function in the spectrum around 1200 MeV (not displayed in Figs. 10 and 11), whereas the higher one lies above the

$\alpha - \pi$ and $\sigma - \eta$ thresholds and roughly corresponds to a broad bump around 1400 MeV in the spectral function [23], see Figs. 10 and 11. The question of the physical meaning of the heavier of the two branches arises, i.e., if actual poles exist on the second (unphysical) Riemann sheet of the S-matrix, that can be associated with this zero in the real part of the inverse propagator [10,23]? This question is more difficult to address, as it demands analytic continuation onto the second Riemann sheet and will be left for a future investigation.

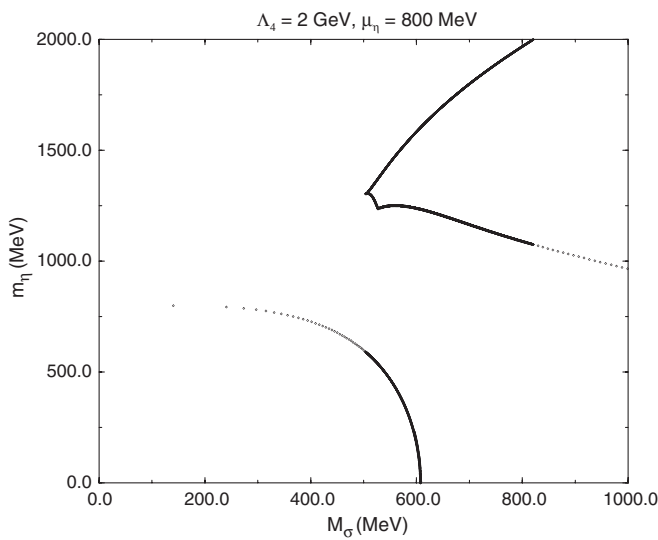


FIG. 8. Isoscalar-pseudoscalar η meson mass (solution to the BS eqs. with $\Lambda_4 = 2$ GeV and $\mu_\eta = 800$ MeV) m_η as a function of the scalar mass M_σ in the 't Hooft model.

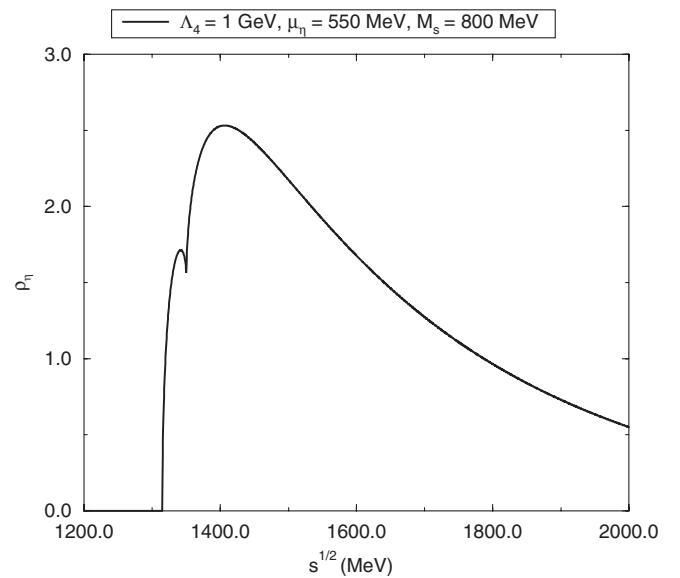


FIG. 10. The Kallen-Lehmann spectral function in the isoscalar-pseudoscalar channel ($\Lambda_4 = 1$ GeV, $\mu_\eta = 550$ MeV and $M_\sigma = 800$ MeV) as a function of the scalar mass $s = (p_1 + p_2)^2$ in the 't Hooft model.

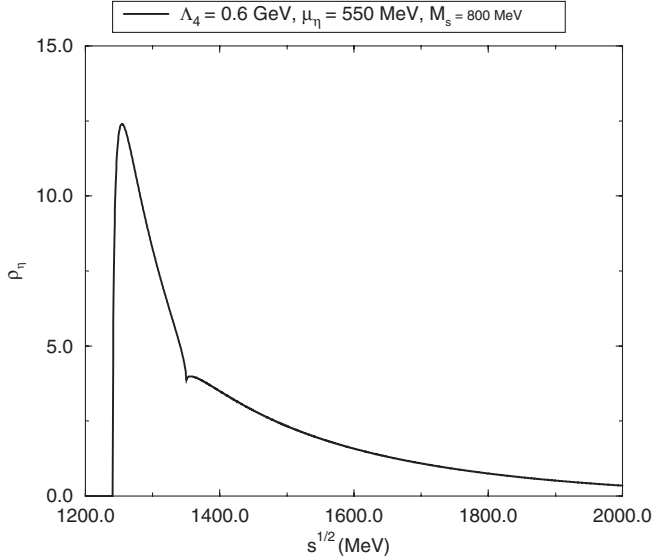


FIG. 11. The Kallen-Lehmann spectral function in the isoscalar-pseudoscalar channel ($\Lambda_4 = 0.6$ GeV, $\mu_\eta = 550$ MeV and $M_\sigma = 800$ MeV) as a function of the scalar mass $s = (p_1 + p_2)^2$ in the 't Hooft model.

Thus we have seen that above some critical value of λ_1 there is one bound and one unbound state in the spectrum. In chiral quark models such as the NJL one, the quartic coupling constant λ_1 can be related to the constituent quark mass m_q by $\lambda_1 = 4m_q^2 f_\pi^{-2}$ [1], thus for sufficiently large constituent quark mass (> 325 MeV) there might be state doubling in the isoscalar-pseudoscalar spectrum. The mass of the heavier state is comparable to, or higher than the cutoff Λ value, however, thus leaving it open to questions.

V. SUMMARY AND CONCLUSIONS

In summary, we have: 1) constructed a unitary, Lorentz and chirally invariant, self-consistent variational approximation to the 't Hooft linear σ model; 2) solved the coupled self-consistent equations of motion in this, the mean-field plus random phase approximation (MFA + RPA). 3) shown that the particle content of the mean-field plus random phase approximation to the 't Hooft linear sigma model is the same as in the Born approximation in the weak coupling limit, i.e., there are four quasi-Goldstone bosons (π , η) and four scalar states, in the weak coupling limit. 4) found that the pions' mass is fixed at the measured value (140 MeV), as a consequence of the validity of Dashen's relation in the MFA + RPA, whereas the isoscalar-pseudoscalar η meson's mass and width can be substantially changed as compared with the Born values, depending on the (free) coupling parameters. 5) calculated the nonperturbative η meson mass by solving the Bethe-Salpeter equation. We found a second and even a

third solution at higher values of mass and coupling; their physical meaning is unclear at this moment.

We did not attempt to address the issues of vacuum stability and high-energy behavior (triviality) of spinless field theories in GA because the 't Hooft model is an effective field theory describing the interactions of mesons as bound states of quarks and antiquarks in the low-energy limit [1]. We have assumed that QCD, i.e., not the ϕ^4 interaction, controls the physics at high energies and thus ensures the stability of the vacuum. The transition from the meson to the QCD d.o.f. is supposed to be mimicked by the cutoff Λ . We have checked that our basic results do not disappear as one increases the value of the Λ/μ_η ratio.

Thus we have shown that the Gaussian variational approximation to the 't Hooft model produces two additional bound/resonant states in the isoscalar-pseudoscalar meson spectrum, depending on the quartic meson coupling strength, or equivalently on the constituent quark mass in the underlying chiral quark model. The masses of these states are comparable to, or larger than the value of the cutoff Λ , however, thus leaving them questionable as physical predictions. A similar mechanism, if it turns out to be independent of the cutoff, might help shine light on the nature of the $f_0(980)$ and $a_0(980)$ mesons in more realistic models. That task remains for the future, however.

The mean-field approximation (MFA), or Gaussian method was initially fraught with problems when applied to the linear σ model with spontaneously broken internal symmetry—the Goldstone theorem did not seem to work. This problem was solved in Ref. [21]: The Goldstone boson found in the Gaussian approximation turned out to be a composite massless state, just as in the NJL model. Yet, there seemed to exist another massive state with the quantum numbers of the pion. That was so only in appearance: there is no pole in the propagator corresponding to this “particle”.

The MFA to the purely bosonic linear σ model is significantly different from the (purely fermionic) NJL one in one regard: Whereas in the NJL model the gap equation “dresses” the fermions and the BS equation describes mesons as bound states of dressed fermions, in the linear σ model both the gap and the BS equations “dress” mesons in two different ways: 1) the gap equations involves one-particle reducible “cactus” diagrams that produce only a momentum-independent self-energies/masses; 2) the BS equations involves one-particle irreducible diagrams that produce only momentum-dependent self-energies. But the traces of the first dressing remain in the theory even after the second dressing has been implemented and this fact has led to some confusion about the particle content of this approximation. An even more complicated situation occurs in the scalar meson sector. We hope to extend these calculations to physical applications in the more realistic SU(3) symmetric Lagrangian in the future.

ACKNOWLEDGMENTS

This work was done while the first author (I. N.) was an M.Sc. student at RCNP, Osaka University, but the present material was not included in this author's M.Sc. thesis. The other author (V. D.) would like to acknowledge a center-of-excellence (COE) professorship and the hospitality of RCNP during the school year 2000/1 when this work was started. We wish to acknowledge kind help in all matters concerning computers and software that we received from Ms. Miho Takayama-Koma. The authors also wish to acknowledge Professor H. Toki for enabling this collaboration.

APPENDIX A: THE ISOVECTOR-PSEUDO-SCALAR SECTOR BETHE-SALPETER EQUATION

The BS eq for $D_{\sigma\eta}$

$$\begin{aligned} D_{\sigma\pi}^{ij}(s) &= V_{\sigma\pi}^{ij}(s) + V_{\sigma\pi}^{il}(s)\Pi_{\sigma\pi}^{lm}(s)D_{\sigma\pi}^{mj}(s) \\ &\quad + V_{\sigma\eta;\pi a}(s)^{il}\Pi_{\eta a}^{lm}(s)D_{\sigma\pi;\eta a}^{mj}(s) \\ &= V_{\sigma\pi}(s)\delta^{ij} + V_{\sigma\pi}(s)\Pi_{\sigma\pi}(s)D_{\sigma\pi}^{ij}(s) \\ &\quad + V_{\sigma\eta;\pi a}(s)\Pi_{\eta a}(s)D_{\sigma\pi;\eta a}^{ij}(s), \end{aligned} \quad (\text{A1})$$

where

$$V_{\sigma\pi}^{ij}(s) = -\lambda_1 \left[1 + \frac{\lambda_1 v^2}{s - \mu_\pi^2} \right] \delta^{ij}$$

and

$$V_{\sigma\pi;\eta a}^{ij}(s) = -\lambda_2 \left[1 + \frac{\lambda_1 v^2}{s - \mu_\pi^2} \right] \delta^{ij} = \frac{\lambda_2}{\lambda_1} V_{\sigma\pi}(s)$$

Take the isospin indices equal to 1, $i = j = 1$ (without summation) to find the solution

$$D_{\sigma\pi;\eta a}^{(11)}(s) = \frac{-V_{\sigma\pi}(s) + (1 - V_{\sigma\pi}(s)\Pi_{\sigma\pi}(s))D_{\sigma\eta}(s)}{V_{\sigma\pi;\eta a}(s)\Pi_{\eta a}(s)}, \quad (\text{A2})$$

Similarly we may set up BS eqs for $D_{\sigma\pi;\eta a}$:

$$\begin{aligned} D_{\sigma\pi;\eta a}^{ij}(s) &= V_{\sigma\pi;\eta a}^{ij}(s) + V_{\sigma\pi;\eta a}^{il}(s)\Pi_{\sigma\pi}^{lm}(s)D_{\sigma\pi}^{mj}(s) \\ &\quad + V_{\eta a}(s)^{il}\Pi_{\eta a}^{lm}(s)D_{\sigma\pi;\eta a}^{mj}(s) \\ &= V_{\sigma\pi;\eta a}(s)\delta^{ij} + V_{\sigma\pi;\eta a}(s)\Pi_{\sigma\pi}(s)D_{\sigma\pi}^{ij}(s) \\ &\quad + V_{\eta a}(s)\Pi_{\eta a}(s)D_{\sigma\pi;\eta a}^{ij}(s), \end{aligned} \quad (\text{A3})$$

where

$$V_{\sigma\pi;\eta a}^{ij}(s) = -\lambda_2 \left[1 + \frac{\lambda_1 v^2}{s - \mu_\pi^2} \right] \delta^{ij} = \frac{\lambda_2}{\lambda_1} V_{\sigma\pi}^{ij}(s)$$

and

$$V_{\eta a}^{ij}(s) = -\lambda_2 \left[1 + \frac{\lambda_2 v^2}{s - \mu_\pi^2} \right] \delta^{ij}.$$

Take the isospin indices equal to 1, $i = j = 1$ (without summation):

$$\begin{aligned} D_{\sigma\eta;\pi a}^{11}(s) &= V_{\sigma\eta;\pi a}(s) + V_{\sigma\pi;\eta a}(s)\Pi_{\sigma\pi}(s)D_{\sigma\pi}^{11}(s) \\ &\quad + V_{\eta a}(s)\Pi_{\eta a}(s)D_{\sigma\pi;\eta a}^{11}(s) \\ &= \frac{\lambda_2}{\lambda_1} V_{\sigma\pi}(s)(1 + \Pi_{\sigma\pi}(s)D_{\sigma\pi}^{11}(s)) \\ &\quad + V_{\eta a}D_{\sigma\eta;\pi a}^{11}(s)\Pi_{\eta a}(s), \end{aligned} \quad (\text{A4})$$

to find the solution

$$D_{\sigma\eta;\pi a}^{11}(s) = \frac{\frac{\lambda_2}{\lambda_1} V_{\sigma\pi}(s)(1 + \Pi_{\sigma\pi}(s)D_{\sigma\pi}^{11}(s))}{1 - V_{\eta a}(s)\Pi_{\eta a}(s)}, \quad (\text{A5})$$

Insert Eq. (A5) into Eq. (A2) to obtain an equation for $D_{\sigma\pi}(s)$ with the solution:

$$D_{\sigma\pi}^{-1}(s) = \frac{(1 - V_{\sigma\pi}(s)\Pi_{\sigma\pi}(s))(1 - V_{\eta a}(s)\Pi_{\eta a}(s)) - V_{\sigma\pi;\eta a}(s)\Pi_{\eta a}(s)\Pi_{\sigma\pi}(s)\frac{\lambda_2}{\lambda_1} V_{\sigma\pi}(s)}{V_{\sigma\pi;\eta a}(s)\Pi_{\eta a}(s)\frac{\lambda_2}{\lambda_1} V_{\sigma\pi}(s) + V_{\sigma\pi}(s)(1 - V_{\eta a}(s)\Pi_{\eta a}(s))}, \quad (\text{A6})$$

In order to extract the pole mass (position) we multiply the numerator in Eq. (A6) which is just the discriminant of this system of linear equations by $(s - \mu_\pi^2)$ and then look for the zeros, usually around $s \simeq 0$:

$$(s - M^2)\mathcal{D}_{\sigma\pi}(s) = 0. \quad (\text{A7})$$

APPENDIX B: THE ISOSCALAR-PSEUDO-SCALAR SECTOR BETHE-SALPETER EQUATION

The BS eq for $D_{\sigma\eta}$

$$\begin{aligned}
D_{\sigma\eta}(s) &= V_{\sigma\eta}(s) + V_{\sigma\eta}(s)\Pi_{\sigma\eta}(s)D_{\sigma\eta}(s) \\
&\quad + V_{\sigma\eta;\pi a}(s)^{ik}\Pi_{\pi a}^{ijkl}(s)D_{\sigma\eta;\pi a}^{jl}(s) \\
&= V_{\sigma\eta}(s) + V_{\sigma\eta}(s)\Pi_{\sigma\eta}(s)D_{\sigma\eta}(s) \\
&\quad + V_{\sigma\eta;\pi a}(s)\delta^{ik}\Pi_{\pi a}\delta^{ij}\delta^{kl}(s)D_{\sigma\eta;\pi a}\delta^{jl}(s) \\
&= V_{\sigma\eta}(s) + V_{\sigma\eta}(s)\Pi_{\sigma\eta}(s)D_{\sigma\eta}(s) \\
&\quad + 3V_{\sigma\eta;\pi a}(s)\Pi_{\pi a}(s)D_{\sigma\eta;\pi a}^{(0)}(s), \tag{B1}
\end{aligned}$$

where

$$V_{\sigma\eta}(s) = -\lambda_1 \left[1 + \frac{\lambda_1 v^2}{s - \mu_\eta^2} \right]$$

and

$$V_{\sigma\eta;\pi a}^{ik}(s) = -\lambda_2 \left[1 + \frac{\lambda_1 v^2}{s - \mu_\eta^2} \right] \delta^{ik} = \frac{\lambda_2}{\lambda_1} V_{\sigma\eta}(s) \delta^{ik}$$

with the solution

$$D_{\sigma\eta;\pi a}^{(0)}(s) = \frac{-V_{\sigma\eta}(s) + (1 - V_{\sigma\eta}(s)\Pi_{\sigma\eta}(s))D_{\sigma\eta}(s)}{3V_{\sigma\eta;\pi a}(s)\Pi_{\pi a}(s)}, \tag{B2}$$

Similarly we may set up BS eqs for $D_{\sigma\eta;\pi a}$:

$$\begin{aligned}
D_{\sigma\eta;\pi a}^{ij}(s) &= V_{\sigma\eta;\pi a}^{ij}(s) + V_{\sigma\eta;\pi a}^{ij}(s)\Pi_{\sigma\eta}(s)D_{\sigma\eta}(s) \\
&\quad + V_{\pi a;\pi a}(s)^{ijkl}\Pi_{\pi a}^{kmnl}(s)D_{\sigma\eta;\pi a}^{mn}(s) \\
&= V_{\sigma\eta;\pi a}^{ij}(s) + V_{\sigma\eta;\pi a}^{ij}(s)\Pi_{\sigma\eta}(s)D_{\sigma\eta}(s) \\
&\quad + V_{\pi a;\pi a}(s)^{ijkl}D_{\sigma\eta;\pi a}^{kl}(s)\Pi_{\pi a}(s), \tag{B3}
\end{aligned}$$

Project out the isoscalar component:

$$\begin{aligned}
D_{\sigma\eta;\pi a}^{(0)}(s) &= V_{\sigma\eta;\pi a}(s) + V_{\sigma\eta;\pi a}(s)\Pi_{\sigma\eta}(s)D_{\sigma\eta}(s) \\
&\quad + V_{\pi a;\pi a}(s)^{iikl}D_{\sigma\eta;\pi a}^{kl}(s)\Pi_{\pi a}(s) \\
&= V_{\sigma\eta;\pi a}(s) + V_{\sigma\eta;\pi a}(s)\Pi_{\sigma\eta}(s)D_{\sigma\eta}(s) \\
&\quad + \left(-(\lambda_1 + \lambda_2) + 3\lambda_2 \left[1 - \frac{\lambda_2 v^2}{s - \mu_\eta^2} \right] \right) \\
&\quad \times D_{\sigma\eta;\pi a}^{(0)}(s)\Pi_{\pi a}(s), \tag{B4}
\end{aligned}$$

$$D_{\sigma\eta;\pi a}^{(0)}(s) = \frac{V_{\sigma\eta;\pi a}(s)(1 + V_{\sigma\eta}(s)\Pi_{\sigma\eta}(s))D_{\sigma\eta}(s)}{1 - Y_{\sigma\eta;\pi a}(s)\Pi_{\pi a}(s)}, \tag{B5}$$

Insert Eq. (B5) into Eq. (B2) to obtain an equation for $D_{\sigma\eta}(s)$ with the solution:

$$D_{\sigma\eta}^{-1}(s) = \frac{(1 - Y_{\sigma\eta;\pi a}(s)\Pi_{\pi a}(s))(1 - V_{\sigma\eta}(s)\Pi_{\sigma\eta}(s)) - 3V_{\sigma\eta}^2(s)\Pi_{\sigma\eta}(s)\Pi_{\pi a}(s)}{V_{\sigma\eta}(s)(1 + 3V_{\sigma\eta}(s)\Pi_{\sigma\eta}(s) - Y_{\sigma\eta;\pi a}(s)\Pi_{\pi a}(s))}, \tag{B6}$$

In order to extract the pole mass (position) we multiply this by $(s - \mu_\eta^2)$ and then look for the zeros.

-
- [1] V. Dmitrašinović, *Phys. Rev. C* **53**, 1383 (1996).
[2] B.W. Lee, *Chiral Dynamics* (Gordon and Breach, New York, 1972).
[3] T. Barnes and G.I. Ghandour, *Phys. Rev. D* **22**, 924 (1980); see also *Variational Calculations in Quantum Field Theory*, edited by L. Polley and D.E.L. Pottinger (World Scientific, Singapore, 1987).
[4] J.L. Basdevant and B.W. Lee, *Phys. Rev. D* **2**, 1680 (1970); K.S. Jhung and R.S. Willey, *Phys. Rev. D* **9**, 3132 (1974); W. Lin and B. Serot, *Nucl. Phys. A* **512**, 650 (1990).
[5] S. Chiku and T. Hatsuda, *Phys. Rev. D* **57**, R6 (1998); *Phys. Rev. D* **58**, 076001, (1998); H.-S. Roh, and T. Matsui, *Eur. Phys. J. A* **1**, 205 (1998); Y. Nemoto, K. Naito, and M. Oka, *Eur. Phys. J. A* **9**, 245 (2000).
[6] A.K. Kerman and Chi-Yong Lin, *Ann. Phys. (N.Y.)* **269**, 55 (1998).
[7] Z. Aouissat, O. Bohr, and J. Wambach, *Mod. Phys. Lett. A* **13**, 1827 (1998).
[8] R.J. Rivers, *Path Integral Methods in Quantum Field Theory* (Cambridge University Press, Cambridge, 1987); B. Hatfield, *Quantum Field Theory of Point Particles and Strings* Addison-Wesley, Reading, 1992).
[9] J.M. Cornwall, R. Jackiw, and E. Tomboulis, *Phys. Rev. D* **10**, 2428 (1974).
[10] I. Nakamura and V. Dmitrašinović, *Nucl. Phys. A* **713**, 133 (2003).
[11] V. Dmitrašinović and I. Nakamura, *J. Math. Phys. (N.Y.)* **44**, 2839 (2003).
[12] M. Lévy, *Nuovo Cimento A* **52**, 23 (1967).
[13] H.W. Crater, *Phys. Rev. D* **1**, 3313 (1970).
[14] J.T. Lenaghan, D.H. Rischke, and J. Shaeffner-Bielich, *Phys. Rev. D* **62**, 085008 (2000).
[15] H.X. Chen, V. Dmitrašinović, and H. Toki, *Phys. Rev. D* **82**, 034011 (2010).

- [16] G. 't Hooft, *Phys. Rep.* **142**, 357 (1986).
- [17] G. Marx, *Phys. Rev.* **140**, B1068 (1965).
- [18] P.M. Stevenson, *Phys. Rev. D* **32**, 1389 (1985); P.M. Stevenson and R. Tarrach, *Phys. Lett. B* **176**, 436 (1986); P.M. Stevenson, *Z. Phys. C* **35**, 467 (1987).
- [19] P.M. Stevenson, B. Allès, and R. Tarrach, *Phys. Rev. D* **35**, 2407 (1987).
- [20] M. Gell-Mann and M. Levy, *Nuovo Cimento* **16**, 705 (1960).
- [21] V. Dmitrašinović, J.R. Shepard, and J.A. McNeil, *Z. Phys. C* **69**, 359 (1996).
- [22] I. Nakamura and V. Dmitrašinović, *Prog. Theor. Phys.* **106**, 1195 (2001).
- [23] V. Dmitrašinović, *Phys. Lett. B* **433**, 362 (1998).